RSC Advances

PAPER

View Article Online
View Journal | View Issue

Cite this: *RSC Adv.*, 2016, **6**, 14563

Silver nanoparticles as highly efficient and selective optical probe for sulphide *via* dendrimer formation in aqueous medium†

Isha Sanskriti and K. K. Upadhyay*

We herein report a highly efficient, cost effective, convenient as well as selective colorimetric probe for sulphide (S^{2-}) in the form of silver nanoparticles (AgNPs) capped by an azonaphthol *viz.* 1-[(4-nitrophenyl)azo]-2-naphthol. A naked eye color change from bright yellow to colorless was observed upon the addition of S^{2-} to the AgNPs. A remarkable feature of this probe is the unique morphological transition of spherical AgNPs to dendritic architecture induced by S^{2-}. Although dendritic AgNPs have been reported previously also by many workers through various methods. Here we are presenting a probe that not only selectively recognises S^{2-} colorimetrically but at the same time paves the way for the self-assembled dendritic structure of AgNPs. The lowest detection limit for S^{2-} was found to be 67 nM which is much lower than the maximum endurable level (15 μM) of S^{2-} in drinking water by World Health Organisation (WHO).

Received 2nd December 2015
Accepted 24th January 2016

DOI: 10.1039/c5ra25625a

www.rsc.org/advances

Introduction

Metal nanoparticles have successfully been explored for their applications in biological, biomedical, chemical and analytical fields.[1,2] On one hand they are utilized for diagnosis, therapeutics[3] and imaging[4,5] purposes, while on the other hand they have also been widely used in perceiving a wide spectrum of analytes ranging from ions, small molecules to biomolecules.[6,7] Their applicability as chemical sensors is widely been exploited due to their size, shape and morphology dependent optical properties.[8] The occurrence of a Surface Plasmon Resonance (SPR) band in the UV-visible range and its modulation by different analyte in their characteristic way paved the way for their uses in analyte sensing.[8–10]

Among metal nanoparticles, gold (Au) and silver (Ag) nanoparticles (NPs) have widely been used in the field of analyte recognition as their sensing response can be easily observed through naked eye.[11] Furthermore, AgNPs being less obnoxious with additional features of simple manageability, biocompatibility, high selectivity and sensitivity have attracted a number of researchers towards their use as optical sensors.[8,12–14] We have concentrated on AgNPs as the same have high extinction coefficient as compared to AuNPs of the same size,[11,12,14,15] as well as exhibit better naked eye response.[15] At the same time they are cost effective also as compared to AuNPs.[15]

Detection of S^{2-} is important from environmental point of view as the same is toxic and gets converted into obnoxious H_2S at physiological pH in the living systems.[16] Natural as well as waste water are very common sources of S^{2-}.[16–18] Humans are vulnerable to high concentration of S^{2-} increasing the risks of respiratory arrest, loss of consciousness and discomfort in mucous membranes.[19] So its detection has become a matter of serious concern for environment as well as for human health.

Various colorimetric and fluorescent molecular probes for sulphide have been reported in the literature but most of them suffer with one or other bottlenecks. The biggest bottleneck is the tedious synthesis of molecular probes and their detection limits.[20–27] Only a few worthy probes are available till date.[28,29] In this context the NPs are better candidates and a number of such types of probes for sulphide have been reported till date. A few among these are CuNPs, Cu@AuNPs, glutathione modified AuNPs, Au/Ag core/shell NRs (nanorods), unmodified Au@Ag nanoclusters, and citrate capped AuNPs.[16,30–34] The LOD's of these probes were of micromolar level. Hence they are not very promising ones. A DNA-templated CuNPs and a citrate capped AuNPs with nanomolar detection limit have also been reported in literature.[35,36] Hence, under these circumstances the AgNPs being reported through this communication as a sensor for S^{2-} with LOD of 67 nM is certainly a worth full report. The non-interference with a large number of anions further makes our report even more worthy and lucrative.

A further literature survey related to NPs revealed that their morphology also affect their properties a lot.[37,38] Hence a variety of nanostructures like nanotrees, nanopines, nanopalms, nanoleaves, nanoforests, nanobushes, nanomushrooms, nanoflowers, nanobouquets, nanomulberry, nanograss,

---

Department of Chemistry (Centre of Advanced Study), Faculty of Science, Banaras Hindu University, Varanasi 221005, India. E-mail: drkaushalbhu@yahoo.co.in; kku@bhu.ac.in; Tel: +91-542-6702488

† Electronic supplementary information (ESI) available: Synthesis, ^1H & ^{13}C NMR, IR and HRMS of CA has been given. See DOI: 10.1039/c5ra25625a

nanokelps, nanocorns, nanocactus, nanospines, nanosheafs have been synthesised.[39] Dendritic AgNPs with multidirectional branches and showing association between different parts have attracted a lot of interest.[37] Furthermore a number of dendritic nanostructures have also been synthesized by involving a number of reductant/surfactant[38,40] and also through various synthetic protocols.[41–45] None of these methods served the purpose of analyte sensing.

On the contrary to above reports, our present report incorporates the S^{2-} specific aggregation of AgNPs as dendrimer which also served the purpose of S^{2-} sensing through the naked eye color change.

Experimental

Materials and methods

All the reagents and solvents were of AR-grade quality and were used as received. The *para*-nitroaniline, β-naphthol, $NaNO_2$, and $AgNO_3$ were purchased from Sigma Aldrich. Stock solutions of the anions and cations were prepared freshly in Milli-Q water. All the spectroscopic studies were made after appropriate dilution. All the glasswares were properly cleaned with freshly prepared aqua regia (3 : 1, (v/v) $HCl–HNO_3$) and finally rinsed many times with Milli-Q water prior to their uses.

Physical measurements

The ^1H NMR and ^{13}C NMR spectra for the same were recorded in $CDCl_3$ with a JEOL AL 300 FT NMR spectrometer. The IR spectra was recorded with a Perkin-Elmer spectrometer. High resolution mass spectroscopy (HRMS) was recorded on a Thermo Scientific Q-Exactive, Accela 1250 pump. Electronic spectra were recorded at room temperature (298 K) on a UV-1800 Pharmaspec spectrophotometer with quartz cuvette (path length = 1 cm). TEM (transmission electron microscope) studies were carried out using FEI, TECNAI 20 G^2 operating at 200 kV. SEM (scanning electron microscope) studies were done using FEI, Quanta-200. AFM (atomic force microscope) studies were carried out using NT-MDT, Solver Next.

Synthesis of the capping agent 1-[(4-nitrophenyl)azo]-2-naphthol, (CA)

Para-nitroaniline (1.38 g, 0.01 mol) was dissolved in a mixture of concentrated HCl (5.0 mL) and distilled water (20 mL) in a round bottom flask. A cold solution of ($NaNO_2$) sodium nitrite (0.83 g, 0.012 mol) in distilled water (5.0 mL) was added dropwise to the acidic solution of *para*-nitroaniline maintained at 0 °C over a time period of ~5 min. The reaction mixture was further stirred at 0 °C for ~40 min followed by addition of cooled solution of β-naphthol (1.44 g, 0.01 mol) in 20 mL of NaOH (4 g, 0.1 mol). The reaction mixture was further stirred for 1 hour. An orange colored product was precipitated and was filtered on suction pump, washed several times with water and finally dried over anhydrous $CaCl_2$ in a desiccator (ESI; Scheme 1†). The structure of the capping agent (CA) thus synthesized is shown in Fig. 1.

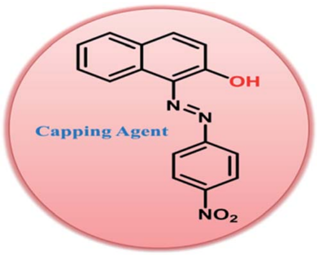

Fig. 1 Structure of the capping agent (CA).

CA was characterized by ^1H, ^{13}C NMR, IR and mass spectral studies (ESI; Fig. S1–S4†); yield: 88%; ^1H NMR (300 MHz, $CDCl_3$, 298 K, TMS): δ ppm = 16.13 (s, 1H, OH), 8.42–8.40 (d, 2H, Ar–H), 8.33–8.30 (d, 1H, Ar–H), 7.70–7.43 (m, 6H, Ar–H), 6.71–6.67 (d, 1H, Ar–H); ^{13}C NMR (75 MHz, $CDCl_3$, 298 K, TMS): δ ppm = 180.22, 173.93, 155.23, 147.92, 143.55, 129.79, 129.17, 128.63, 127.59, 126.35, 125.79, 125.69, 122.58, 122.47, 116.36, 102.91; IR/cm^{-1}: 3427, 3113, 2922, 1624, 1594, 1575, 1554, 1502, 1453, 1401, 1370, 1332, 1258, 1226, 1204, 1153, 1106, 985, 859, 836, 748, 686, 670, 614, 508, 489, 425; HRMS (ESI): *m*/*z* calculated for $C_{16}H_{11}N_3O_3 + H\ [M + H]^+ = 294.0873$, found = 294.0872.

Synthesis of silver nanoparticles (AgNPs)

The 300 μL of 1.0 M NaOH was diluted with 3.0 mL water and the same was used in the synthesis. 40 mL of Milli-Q water was taken in a round bottom flask. Then, 400 μL of CA (4 mM) prepared in chloroform was added to it with continuous stirring. This was followed by the addition of 400 μL of prepared NaOH and 800 μL of $AgNO_3$ (8 mM) to it. Then 800 μL of the same NaOH was added to the stirring mixture at room temperature which corresponds to pH 14. Slight appearance of yellow color reflects the onset of formation of AgNPs. After an hour, yellow color brightens. The stirring at room temperature was continued for overnight for complete functionalization of AgNPs. The functionalized AgNPs were observed as bright yellow in color with no turbidity. The same was centrifuged prior to use and were stored in round bottom flask at room temperature (ESI; Fig. S5†).

A pH variation study was also done in order to have an idea about the optimum pH suitable for AgNPs synthesis. For this purpose we carried out the synthesis of AgNPs at 6, 8, 10 and 14 pH's (ESI; Fig. S6†). We didn't observe any shift in SPR band of AgNPs in terms of λ_{max} which was a clear indication about no significant change in their size.[46,47] Nevertheless the intensity of SPR band as well as peak area got increased with increase in pH indicating increase in the concentration (in terms of number) of AgNPs.

Photophysical studies of AgNPs with different analyte

A variety of anionic analytes were screened separately for their photophysical (sensing) studies against freshly prepared AgNPs. The photophysical studies were done through naked eye followed by UV-visible studies. The UV-visible titration was performed after each aliquot addition of much lower *i.e.* 1.0×10^{-4}

M concentration of S^{2-} to the 3 mL of AgNPs prepared by diluting 1 mL of AgNPs with 2 mL of Milli-Q water. The colorimetric sensing ability of AgNPs was investigated by separate addition of much higher concentration *i.e.* 10 μL of 1.0×10^{-1} M of anions (F^-, Cl^-, Br^-, I^-, S^{2-}, ($C_6H_5COO^-$) BzO^-, (CH_3COO^-) AcO^-, SO_3^{2-}, SO_4^{2-}, HSO_4^-, $S_2O_5^{2-}$, $S_2O_3^{2-}$) to 1 mL of AgNPs diluted with 2 mL of Milli-Q water.

Interference study

The interference study for the anions was performed at their individual level. To a solution of 1.0 mL AgNPs diluted with 2.0 mL of Milli-Q water, the 10 μL of 1.0×10^{-1} M of different anions (F^-, Cl^-, Br^-, I^-, S^{2-}, BzO^-, AcO^-, SO_3^{2-}, SO_4^{2-}, HSO_4^-, $S_2O_5^{2-}$, $S_2O_3^{2-}$) were added separately followed by addition of the 10 μL of 1.0×10^{-1} M sulphide to each case. The matrix studies with the mixture (10 μL of 1.0×10^{-1} M) of anions and cations (Na^+, K^+, Ba^{2+}, Cr^{3+}, Zn^{2+}, Cd^{2+}, Hg^{2+}, Fe^{3+}, Co^{2+}, Ni^{2+}, Cu^{2+}) separately were also performed to see the effect of sulphide over AgNPs.

Results and discussion

UV-visible characterization of the CA and AgNPs stabilised by it

The absorption spectra of the capping agent (CA) showed a sharp band at 328 nm and broad band at 429 nm and 461 nm. The capped AgNPs as synthesised above appeared bright yellow colored with a corresponding sharp SPR band at 409 nm (Fig. 2).

Interaction of AgNPs with analytes

The above AgNPs were also interacted with a set of cations (10 μL of 1.0×10^{-1}M) *viz.* Na^+, K^+, Ba^{2+}, Cr^{3+}, Zn^{2+}, Cd^{2+}, Hg^{2+}, Fe^{3+}, Co^{2+}, Ni^{2+}, Cu^{2+} for their possible photochemical interaction. No conclusive changes were observed either colorimetrically or in its UV-visible spectrum (ESI; Fig. S7†). So, we switched on to checking the response of AgNPs with anions (F^-, Cl^-, Br^-, I^-, S^{2-}, BzO^-, AcO^-, SO_3^{2-}, SO_4^{2-}, HSO_4^-, $S_2O_5^{2-}$, $S_2O_3^{2-}$) and found that the bright yellow colored AgNPs underwent bleaching upon the interaction of S^{2-} only and the corresponding UV-visible spectrum showed the disappearance of SPR band at 409 nm and slight broadening of the band is also observed (Fig. 3).

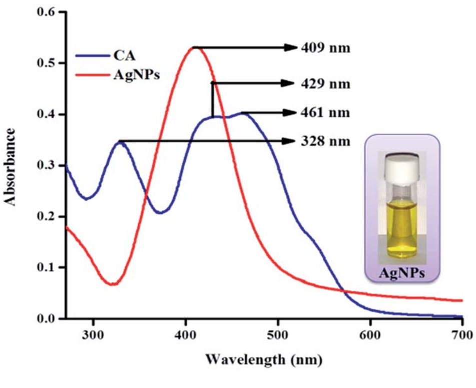

Fig. 2 UV-visible spectrum of the capping agent (CA) and AgNPs.

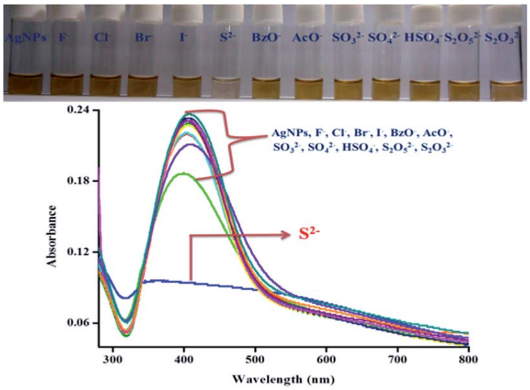

Fig. 3 Naked eye response and the corresponding UV-visible spectrum of capped AgNPs in absence and presence of different anions (10 μL of 1.0×10^{-1} M).

No interference was observed by any anion in the presence of S^{2-} either in naked eye or in the UV-visible spectrum pattern (ESI; Fig. S8†). The plot of A_{409} of capped AgNPs in the mixture of S^{2-} with other anions reflects the interference study (Fig. 4).

In the matrix studies of anions, the addition of all anions to AgNPs resulted in almost insignificant visual change. The addition of S^{2-} to this mixture led to bleaching of yellow color of AgNPs. The same was also reflected in the UV-visible spectral studies. This clearly proves the efficient applicability of this probe for the visual sensing of sulphide in the mixture of a vast number of anions (ESI; Fig. S9†).

Addition of the mixture of a large number of cations to AgNPs resulted in bleaching of yellow color of AgNPs. Nevertheless, addition of S^{2-} to the same mixture lead to revival of slight yellow color with its reflection in the UV-visible spectrum (ESI; Fig. S10†).

Detection of S^{2-} and analytical data

The UV-visible titration was performed with S^{2-} at different concentration (0 to 43.89 μM) showing gradual disappearance of SPR band at 409 nm and slow broadening of the same. Same

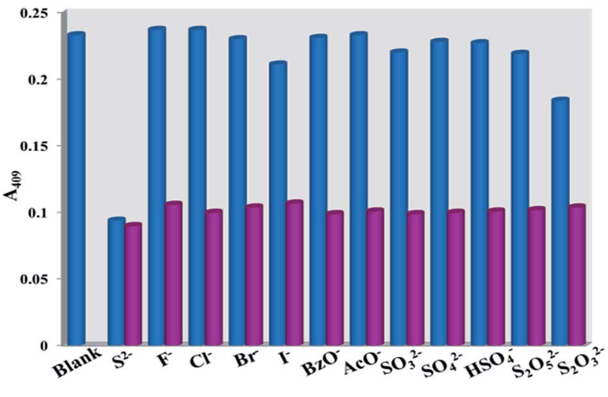

Fig. 4 Interference study of AgNPs with various anions; blue bars: AgNPs + anions, purple bars: AgNPs + anions + S^{2-}.

was translated in the form of bleaching of color of AgNPs (Fig. 5).

The calibration curve was plotted which was linear in the range from 0.33 μM to 2.64 μM and follows the linear equation, $y = 0.0242x + 0.0075$ with the value of R^2 equal to 0.9948 (Fig. 6). LOD was calculated from three times the standard deviation of blank signal. The LOD of capped AgNPs for S^{2-} was calculated to be 67 nM.

Stability of AgNPs and its sensing action with respect to pH

As evident from the photographs (ESI; Fig. S11a†) there was slight effect on the bright yellow color of AgNPs at pH 2 and 3. From pH 4 to 10, the color and the SPR band was maintained. So, the AgNPs are very stable within the pH range 4 to 10 with slight less stability at pH 2 and 3. The effectiveness of AgNPs for colorimetric sensing of S^{2-} is in good agreement within the pH range 4 to 10 (ESI; Fig. S11b†). The plot of Absorbance *vs.* pH reflects the same result as discussed (Fig. 7).

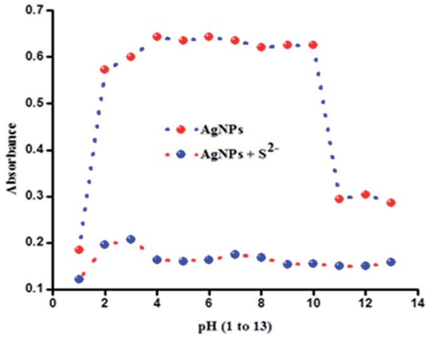

Fig. 7 Stability of AgNPs and its response for sensing S^{2-} from pH 1 to 13.

Probable mechanism of formation of capped AgNPs

The reducing action of phenolic moiety in basic medium is supposed to be responsible for the conversion of Ag^+ to Ag.[13,14,48] The subsequent conversion of naphthoxide ion into naphthoxyl radical in its quinone type structure leads to formation of numerous dimeric structures which are ultimately adsorbed over AgNPs.[13,14] The presence of nitro and diazo groups serve as a tail to stabilize the monodispersed AgNPs. The resulting AgNPs were stable upto 5–6 months at the room temperature. Thus capping agent serves the dual purpose *i.e.* reduction of Ag^+ to Ag as well as stabilizing the AgNPs by getting adsorbed over them. This proposed mechanistic pathway has been given in Scheme 1.

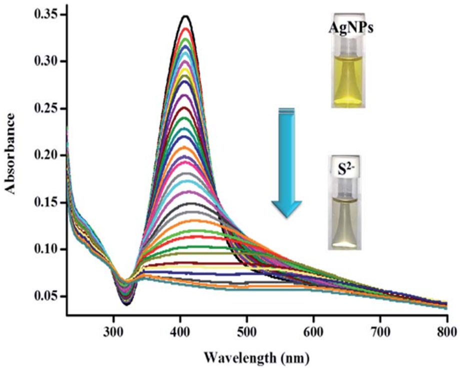

Fig. 5 UV-visible spectrum of AgNPs at different concentration (0 to 43.89 μM) of S^{2-}.

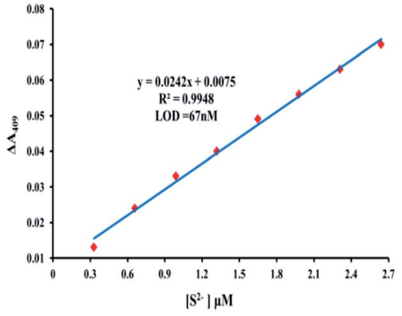

Fig. 6 The calibration curves for capped AgNPs in presence of S^{2-}.

Azonaphthol capped AgNPs appeared bright yellow in color and are spherical in shape and well dispersed as is evident from their TEM image (Fig. 8a). The average size of particle calculated from the TEM image was found to be 10–15 nm. Moreover the SEM and AFM images (Fig. 8b and c) also support the spherical morphology of AgNPs.

Probable mechanism of colorimetric sensing of S^{2-} through AgNPs

The capping agent itself doesn't give any response upon the addition of sulphide to it which is very clearly reflected in the UV-visible spectrum of CA (ESI; Fig. S12†). On the other hand

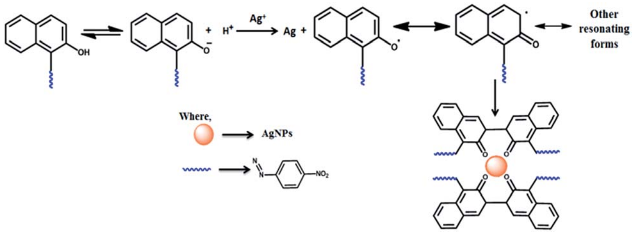

Scheme 1 Probable mechanistic pathway of formation and stabilization of AgNPs by capping agent.

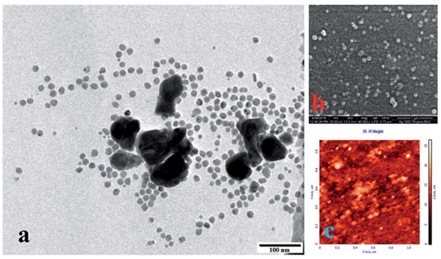

Fig. 8 (a) TEM, (b) SEM, (c) AFM images of capped AgNPs.

the capped AgNPs got transformed into a dendritic architecture which was reflected in the corresponding TEM (Fig. 9a–f) and SEM (Fig. 10a–f) images at their different magnifications. Visually this process was translated in terms of change in color of AgNPs from bright yellow to colorless which was further supported from the AFM studies also (Fig. 11a and b).

The solution of Na_2S is itself highly alkaline and there is presence of S^{2-} along with HS^- due to hydroxylation of S^{2-}. The latimer diagram for sulphur in basic medium[49] (Fig. 12) suggests an spontaneous conversion of HS^- to S. This sulphur oxidizes metallic silver into silver ion getting itself reduced into sulphide ion. Now the soft–soft interaction between Ag^+ and S^{2-} leads to precipitation of Ag_2S.[50] This mechanism clearly explains the microscopic images of majority of spherical capped-AgNPs coming close together and their some parts getting dissolved in the form of Ag_2S which serves as connectivity between the particles which are arranged in dendritic fashion (Fig. 9f, inset). The EDX studies of the AgNPs (ESI; Fig. S13a†) and its ensemble with sulphide (ESI; Fig. S13b†) clearly indicated the peaks for Ag and Ag as well as sulphur respectively.

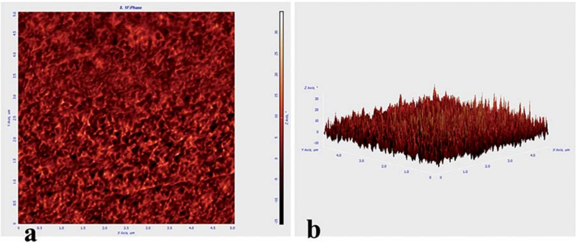

Fig. 11 (a) AFM image of sulphide induced dendrimer formation of AgNPs and (b) 3-D image.

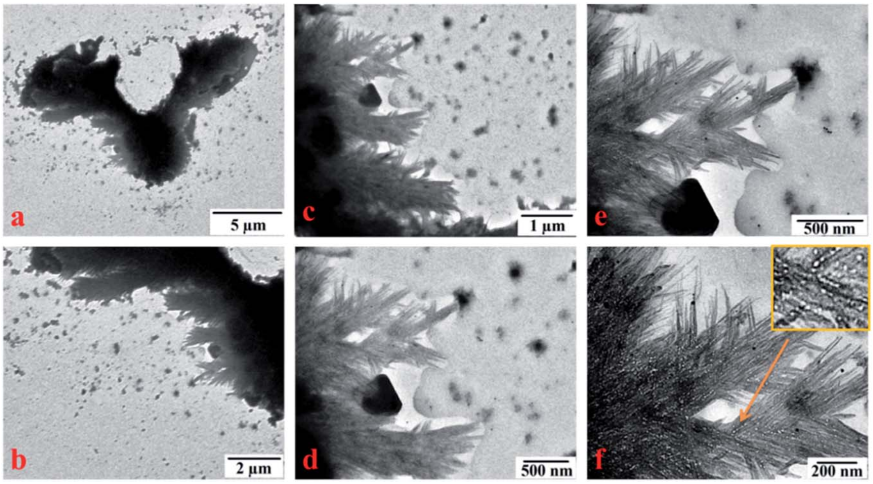

Fig. 9 TEM images of sulphide induced dendrimer formation of AgNPs from lower to higher magnification (a–f).

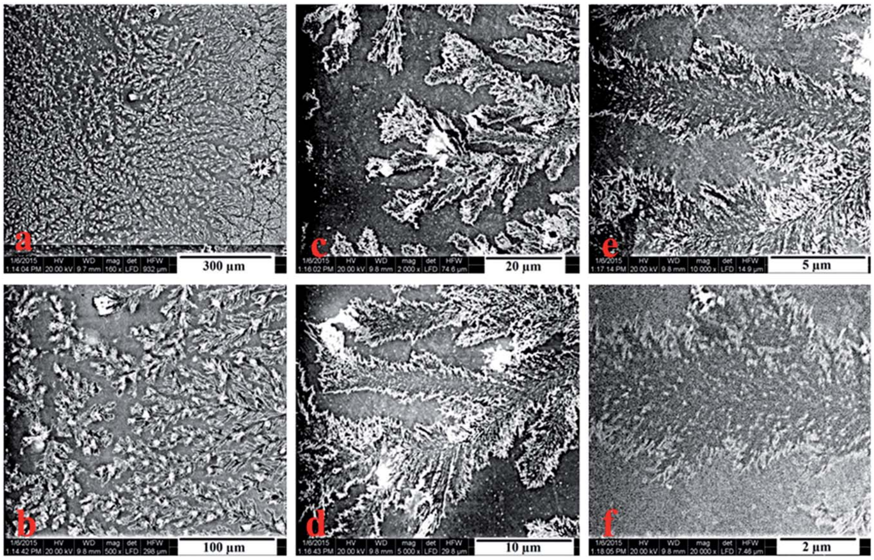

Fig. 10 SEM images of sulphide induced dendrimer formation of AgNPs from lower to higher magnification (a–f).

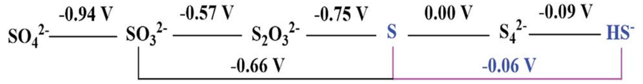

Fig. 12 Latimer diagram of sulphur in basic medium.

Conclusion

Thus 1-[(4-nitrophenyl)azo]-2-naphthol capped AgNPs were conveniently synthesised, characterized and exploited for effective colorimetric sensing of S^{2-} with LOD of 67 nm which is much lower than the sustainable level (15 μM) of S^{2-} in drinking water accepted by WHO.[25] Additional feature of this probe is the beautiful arrangement of spherical AgNPs in dendritic fashion induced by S^{2-}. Moreover our approach does not deal with complex or specific procedures for sensing as well as in the assembly of AgNPs in dendritic architecture. This probe showed a naked eye color change from bright yellow to colorless for S^{2-}. Applicability of the probe in the wide pH range from 4 to 10 makes it more worthy and lucrative. As all the sensing studies were performed in water, hence our probe can successfully be applied in the naked eye sensing of S^{2-} in aqueous medium in the presence of a group of a large number of similar types of anions. The detailed study and utilisation of this mechanism can be used for both sensing as well as for the genesis of even better architecture.

Acknowledgements

I. S. is thankful to UGC-BSR/RFSMS/432 for fellowship. We acknowledge Prof. O. N. Srivastava, Department of Physics, Faculty of Science, Banaras Hindu University for providing the TEM and SEM facility.

Notes and references

1 S. Bothra, J. N. Solanki and S. K. Sahoo, *Sens. Actuators, B*, 2013, **188**, 937–943.
2 T. Asefa, C. T. Duncan and K. K. Sharma, *Analyst*, 2009, **134**, 1980–1990.
3 J. Yang, C. Zhou, C. Liu, Y. Li, H. Liu, Y. Li and D. Zhu, *Analyst*, 2012, **137**, 1446–1450.
4 A. Alizadeh, M. M. Khodaei, Z. Hamidi and M. B. Shamsuddin, *Sens. Actuators, B*, 2014, **190**, 782–791.
5 V. V. Kumar and S. P. Anthony, *Sens. Actuators, B*, 2014, **191**, 31–36.
6 J. Zhang, X. Wang and X. Yang, *Analyst*, 2012, **137**, 2806–2812.
7 Y. Zhang, Y. Leng, L. Miao, J. Xin and A. Wu, *Dalton Trans.*, 2013, **42**, 5485–5490.
8 J. A. Jacob, H. S. Mahal, N. Biswas, T. Mukherjee and S. Kapoor, *Langmuir*, 2008, **24**, 528–533.
9 J. M. Abad, M. Revenga-Parra, T. Garcia, M. Gamero, E. Lorenzo and F. Pariente, *Phys. Chem. Chem. Phys.*, 2011, **13**, 5668–5678.
10 X. Yuan, S. Wen, M. Shen and X. Shi, *Anal. Methods*, 2013, **5**, 5486–5492.
11 Y. Lin, C. Chen, C. Wang, F. Pu, J. Ren and X. Qu, *Chem. Commun.*, 2011, **47**, 1181–1183.
12 S. Chen, H. Gao, W. Shen, C. Lu and Q. Yuan, *Sens. Actuators, B*, 2014, **190**, 673–678.
13 Y.-r. Ma, H.-y. Niu, X.-l. Zhang and Y.-q. Cai, *Chem. Commun.*, 2011, **47**, 12643–12645.
14 Y. Ma, H. Niu, X. Zhang and Y. Cai, *Analyst*, 2011, **136**, 4192–4196.
15 W. Leesutthiphonchai, W. Dungchai, W. Siangproh, N. Ngamrojnavanich and O. Chailapakul, *Talanta*, 2011, **85**, 870–876.
16 A. Hatamie, B. Zargar and A. Jalali, *Talanta*, 2014, **121**, 234–238.
17 W.-Y. Chen, G.-Y. Lan and H.-T. Chang, *Anal. Chem.*, 2011, **83**, 9450–9455.
18 A. Baciu, M. Ardelean, A. Pop, R. Pode and F. Manea, *Sensors*, 2015, **15**, 14526–14538.
19 X. Lou, D. Ou, Q. Li and Z. Li, *Chem. Commun.*, 2012, **48**, 8462–8477.
20 M. Li, Q. Liang, M. Zheng, C. Fang, S. Peng and M. Zhao, *Dalton Trans.*, 2013, **42**, 13509–13515.
21 M.-Q. Wang, K. Li, J.-T. Hou, M.-Y. Wu, Z. Huang and X.-Q. Yu, *J. Org. Chem.*, 2012, **77**, 8350–8354.
22 Y. Fu, Q.-C. Feng, X.-J. Jiang, H. Xu, M. Li and S.-Q. Zang, *Dalton Trans.*, 2014, **43**, 5815–5822.
23 M. Sun, H. Yu, H. Li, H. Xu, D. Huang and S. Wang, *Inorg. Chem.*, 2015, **54**, 3766–3772.
24 B. Sen, M. Mukherjee, S. Pal, K. Dhara, S. K. Mandal, A. R. Khuda-Bukhsh and P. Chattopadhyay, *RSC Adv.*, 2014, **4**, 14919–14927.
25 Y. Huang, D. Ou, C. Wang, C. Huang, Q. Li and Z. Li, *Polym. Chem.*, 2014, **5**, 2041–2049.
26 X. Cao, W. Lin and L. He, *Org. Lett.*, 2011, **13**, 4716–4719.
27 M. G. Choi, S. Cha, H. Lee, H. L. Jeon and S.-K. Chang, *Chem. Commun.*, 2009, 7390–7392.
28 W. Zhang, J. Kang, P. Li, H. Wang and B. Tang, *Anal. Chem.*, 2015, **87**, 8964–8969.
29 G.-J. Mao, T.-T. Wei, X.-X. Wang, S.-y. Huan, D.-Q. Lu, J. Zhang, X.-B. Zhang, W. Tan, G.-L. Shen and R.-Q. Yu, *Anal. Chem.*, 2013, **85**, 7875–7881.
30 J. Zhang, X. Xu, Y. Yuan, C. Yang and X. Yang, *ACS Appl. Mater. Interfaces*, 2011, **3**, 2928–2931.
31 J. Zhang, X. Xu and X. Yang, *Analyst*, 2012, **137**, 1556–1558.
32 H. Huang, Q. Li, J. Wang, Z. Li, X.-F. Yu and P. K. Chu, *Plasmonics*, 2014, **9**, 11–16.
33 Z.-X. Wang, C.-L. Zheng and S.-N. Ding, *RSC Adv.*, 2014, **4**, 9825–9829.
34 H.-H. Deng, G.-W. Wu, X.-Q. Lin, X.-W. Xu, A.-L. Liu, X.-H. Xia and W. Chen, *RSC Adv.*, 2015, **5**, 58574–58579.
35 J. Liu, J. Chen, Z. Fang and L. Zeng, *Analyst*, 2012, **137**, 5502–5505.
36 Q. Gao, Y. Zheng, C. Song, L.-Q. Lu, X.-K. Tian and A.-W. Xu, *RSC Adv.*, 2013, **3**, 21424–21430.
37 M. H. Rashid and T. K. Mandal, *J. Phys. Chem. C*, 2007, **111**, 16750–16760.

38 X. Wang, K. Naka, H. Itoh, S. Park and Y. Chujo, *Chem. Commun.*, 2002, 1300–1301.
39 O. V. Kharissova and B. I. Kharisov, *Ind. Eng. Chem. Res.*, 2010, **49**, 11142–11169.
40 S. Pang, T. Kondo and T. Kawai, *Chem. Mater.*, 2005, **17**, 3636–3641.
41 Q. Zhou, S. Wang, N. Jia, L. Liu, J. Yang and Z. Jiang, *Mater. Lett.*, 2006, **60**, 3789–3792.
42 J. Fang, H. You, P. Kong, Y. Yi, X. Song and B. Ding, *Cryst. Growth Des.*, 2007, **7**, 864–867.
43 L. Gou, M. Chipara and J. M. Zaleski, *Chem. Mater.*, 2007, **19**, 1755–1760.
44 X. Sun and M. Hagner, *Langmuir*, 2007, **23**, 9147–9150.
45 L. Fan and R. Guo, *Cryst. Growth Des.*, 2008, **8**, 2150–2156.
46 L. M. Liz-Marzan, *Langmuir*, 2006, **22**, 32–41.
47 M. Li, S. K. Cushing and N. Wu, *Analyst*, 2015, **140**, 386–406.
48 K. Yoosaf, B. I. Ipe, C. H. Suresh and K. G. Thomas, *J. Phys. Chem. C*, 2007, **111**, 12839–12847.
49 B. M. Mahan and R. J. Myers, *University Chemistry*, Benjamin Cummings, Menlo Park, CA, 1987.
50 C. Levard, B. C. Reinsch, F. M. Michel, C. Oumahi, G. V. Lowry and G. E. Brown, *Environ. Sci. Technol.*, 2011, **45**, 5260–5266.